PHYSICAL REVIEW D VOLUME 31, NUMBER 11 1 JUNE 1985

Measurement of energy-energy correlations in $e^+e^- \rightarrow$ hadrons at $\sqrt{s} = 29$ GeV

E. Fernandez, W. T. Ford, N. Qi, A. L. Read, Jr., and J. G. Smith
Department of Physics, University of Colorado, Boulder, Colorado 80309

T. Camporesi, R. De Sangro, A. Marini, I. Peruzzi, M. Piccolo, and F. Ronga
Laboratori Nazionali di Frascati dell' Istituto Nazionale di Fisica Nucleare, I-00044 Frascati, Rome, Italy

H. T. Blume, R. B. Hurst, J. C. Sleeman, J. P. Venuti, H. B. Wald, and Roy Weinstein
Department of Physics, University of Houston, Houston, Texas 77004

H. R. Band, M. W. Gettner, G. P. Goderre, O. A. Meyer,* J. H. Moromisato, W. D. Shambroom, and E. von Goeler
Department of Physics, Northeastern University, Boston, Massachusetts 02115

W. W. Ash, G. B. Chadwick, S. H. Clearwater,† R. W. Coombes, H. S. Kaye,‡ K. H. Lau, R. E. Leedy, H. L. Lynch, R. L. Messner, L. J. Moss, F. Muller,§ H. N. Nelson, D. M. Ritson, L. J. Rosenberg, D. E. Wiser, and R. W. Zdarko
Department of Physics and Stanford Linear Accelerator Center, Stanford University, Stanford, California 94305

D. E. Groom and Hoyun Lee**
Department of Physics, University of Utah, Salt Lake City, Utah 84112

M. C. Delfino, B. K. Heltsley,†† J. R. Johnson, T. L. Lavine, T. Maruyama, and R. Prepost
Department of Physics, University of Wisconsin, Madison, Wisconsin 53706

(Received 6 August 1984)

The energy-energy correlation cross section for hadrons produced in electron-positron annihilation at a center-of-mass energy of 29 GeV has been measured with the MAC detector at SLAC. The result is corrected for the effects of detector resolution, acceptance, and initial-state radiation. The correlation is measured in two independent ways on the same data sample: the energy weights and angles are obtained either from the energy flow in the finely segmented total absorption calorimeters or from the momenta of charged tracks in the central drift chamber. This procedure helps reduce systematic errors by cross-checking the effects of the detector on the measurement, particularly important because the corrections depend on complex Monte Carlo simulations. The results are compared with the predictions of Monte Carlo models of complete second-order perturbative quantum chromodynamics and fragmentation, with the following conclusions: (1) fitting the asymmetry for large correlation angles gives values for α_S of 0.120 ± 0.006 in perturbation theory, 0.185 ± 0.013 in the Lund string model, and values which vary from 0.105 to 0.140 (± 0.01) in the incoherent jet models, depending on the gluon fragmentation scheme and the algorithm used for momentum conservation; and (2) the string fragmentation model provides a satisfactory description of the measured energy-energy correlation cross section, whereas incoherent jet formation does not.

I. INTRODUCTION

The energy-energy correlation cross section for electron-positron annihilation into hadrons provides a valuable tool for quantitative studies of quantum chromodynamics (QCD) and fragmentation. The correlation cross section $d\Sigma/d\chi$ describes the energy-weighted angular correlation, averaged over many events, as a function of the angle χ between pairs of energy flow parcels. Measurement of $d\Sigma/d\chi$ does not involve any *ad hoc* jet definition or isolation of specific event topologies and therefore opens to scrutiny the nature of hadronic energy flow in terms of internal event angles, without reference to a jet axis or attempting to distinguish between two- and three-jet events. Specific predictions for $d\Sigma/d\chi$ have been made in the context of first-order[1] and second-order[2,3] perturbative QCD, which neglect fragmentation contributions. The effects of gluon emission are emphasized and those of fragmentation are minimized in the asymmetry $\mathcal{A}(\chi)$ of $d\Sigma/d\chi$ about $\chi = 90°$. However, various Monte Carlo models differ on the importance and precise contribution of fragmentation to the observed correlation and its asymmetry, and hence on how the strong coupling constant α_S should be extracted from the data. This situation has led to a variety of approaches to analysis in previous experiments.[4–12]

The energy-energy correlation cross section is given by[1]

$$\frac{d\Sigma}{d\chi}(\chi_k) = \frac{1}{\Delta\chi}\frac{1}{N_{\text{evts}}}\sum_{\text{evts}}\sum_{l \geq m}\epsilon_l\epsilon_m(2-\delta_{lm}) , \qquad (1)$$

where the ϵ_i represent the normalized energy-flow vectors

of the hadrons in any event, satisfying $\sum |\epsilon_i| = 1$ (energy conservation). The first summation in Eq. (1) averages over the N_{evts} hadronic events in the sample, and for each event the second summation includes all unique pairs of ϵ_i's with $<(\epsilon_l,\epsilon_m)=\chi_k \pm (\Delta\chi/2)$, where χ_k are central values of bins with width $\Delta\chi$. The final factor with the Kronecker δ correctly treats self-correlation terms, ensuring the normalization

$$\int_0^\pi \frac{d\Sigma}{d\chi}(\chi)d\chi = 1 \ . \tag{2}$$

The asymmetry $\mathscr{A}(\chi)$ is defined as

$$\mathscr{A}(\chi) \equiv \frac{d\Sigma}{d\chi}(\pi-\chi) - \frac{d\Sigma}{d\chi}(\chi) \ . \tag{3}$$

In this article a high-statistics measurement of $d\Sigma/d\chi$ is presented. The data were collected with the MAC detector, which operates in the PEP electron-positron storage ring at the Stanford Linear Accelerator Center. The analysis uses 65 000 hadronic events collected over a two-year period corresponding to an integrated luminosity of 215 pb^{-1} at $\sqrt{s} = 29$ GeV. The data are compared to calculations based on perturbation theory alone and to predictions of Monte Carlo models which include string and incoherent jet fragmentation as well.

II. APPARATUS AND EVENT SELECTION

The MAC detector[9,13] consists of a 1-m-diameter solenoid coil containing a drift chamber, surrounded by electromagnetic shower detectors, trigger scintillators, magnetized-iron hadron calorimeters, and muon-tracking drift chambers, all covering about 97% of the solid angle. Events trigger the apparatus on the basis of scintillator hits, energy deposition, tracking information, or combinations of these, resulting in high detection efficiency for multihadrons.

The central drift chamber tracks charged particles with 833 drift cells arranged in 10 cylindrical layers at equally spaced radii from 12 to 45 cm. The layers have the rectangular arrays of field and sense wires for each cell oriented alternately parallel and at plus and minus 3° to the beam line to allow measurement of the axial position of the track crossing. Each cell has two closely spaced sense wires to measure the drift distance without right-left ambiguity. In the 0.57-T axial magnetic field the point measurement error of 200 μm corresponds to an inverse momentum resolution of

$$\sigma_{1/p} = 6.5\% \sin\theta \ (\text{GeV}/c)^{-1}$$

for 23°—157° in polar angle θ, and somewhat worse resolution at smaller angles, 17°—23° and 157°—163°, where only 5—9 layers are crossed. The angular resolution in azimuth varies from 0.15°—0.30° and in polar angle from 0.2—1.2°, depending on θ and the number of layers traversed by the particle.

The finely segmented total-absorption calorimeters measure the magnitude and direction of the energy flow for both charged and neutral particles. Central-section barrel shower chambers and hadron calorimeters in a hexagonal geometry measure particle energies at wide angles to the beam; endcaps complete the solid angle coverage down to 10° in polar angle. Layers of proportional wire chambers (PWC's) alternate with 0.25-cm lead absorber in the shower chambers or 2.5-cm iron in the hadron and end-cap calorimeters. The energy resolutions for electromagnetic showers are $\sigma_E = 20\%\sqrt{E \ (\text{GeV})}$ in the central shower chambers and $45\%\sqrt{E}$ in the end caps; the iron calorimeters achieve $\sigma_E \approx 75\%\sqrt{E}$ for hadron cascades. In the central section 1.9° azimuthal segmentation and charge division yield angular resolutions for showers of about 0.7° in ϕ and 1.4° in θ, respectively. Comparable resolutions are attained in the end caps, where wire groupings correspond roughly to polar angle segments and cathode readout gives azimuthal information. The calorimeters are also segmented in depth: the central shower chambers into three groups (from the coil outward) of 7, 10, and 12 lead-PWC layers, the central hadron calorimeter into three equal groupings of 8 iron-PWC layers each, and the end caps into four layers (from the inside outward) of 3, 6, 11, and 8 iron-PWC layers.

The criteria developed to select hadronic events exploit the large solid-angle coverage of the detector while minimizing background contamination. First, three cuts based on the calorimeter energy hits $\mathbf{E}_i = (E_i,\theta_i,\phi_i)$ reject topologies characteristic of backgrounds, particularly two-photon production of hadrons. An event remains in the sample only if the visible energy $E_{\text{vis}} \equiv \sum |\mathbf{E}_i|$ exceeds 12 GeV, the transverse energy component $E_\perp \equiv \sum |\mathbf{E}_i| \sin\theta_i$ is larger than 7.5 GeV, and the net imbalance $|I| \equiv (|\sum \mathbf{E}_i| / E_{\text{vis}})$ is less than 0.65. Next, at least five charged tracks must be reconstructed in the central drift chamber, and the momenta $\mathbf{p}_i$ of all such tracks must sum to $P_{\text{vis}} \equiv \sum |\mathbf{p}_i| > 2$ GeV/c. Visual scanning of the $\sim 10\%$ of the events with marginal visible or transverse energy, imbalance, momentum sum, or "event quality" (defined, for example, by the average number of hits per track in the central drift chamber) eliminates some remaining backgrounds, such as cosmic rays and Bhabha-scattering events with extra tracks. Two-photon rejection is enhanced by discarding events which fail at least two of the more restrictive requirements: $E_{\text{vis}} > 15$ GeV, $E_\perp > 9.1$ GeV, or $I < 0.55$. Approximately 100 000 events survive these cuts, which are identical to those used in a measurement of the total hadronic cross section.[9]

Additional requirements are made for the energy-energy correlation event sample to reduce systematic uncertainties in the measurement. To ensure nearly full containment of all particles within the detector's angular acceptance, the energy flow thrust axis is required to be more than 40° away from the beam line. To discriminate against events with hard initial-state radiation leaving the detector at small angles to the beam (which have large radiative corrections) the component along the beam line of the imbalance vector $\mathbf{I}$ must have magnitude less than 0.25. About 65 000 events pass these tighter cuts. Monte Carlo studies show that together all the criteria accept about 50% of the total cross section, and admit only 2% background into the sample.

III. MODELS

General arguments[1] can be made that the energy-energy correlations for two-jet fragmentation are dominantly symmetric about $\chi=90°$. A naive approach to extracting the strong coupling constant, then, is to assume *a priori* that all fragmentation effects, including those from the gluon, vanish in the asymmetry for large correlation angles, and hence that the asymmetry of the hadrons is the asymmetry of the partons. In this case, α_S can be directly obtained from the observed asymmetry by fitting it to the second-order perturbative QCD result

$$\mathscr{A}_2(\chi)\equiv\mathscr{A}_1(\chi)\left[1+\frac{\alpha_S}{\pi}G(\chi)\right], \tag{4}$$

where the first-order asymmetry

$$\mathscr{A}_1(\chi)\equiv Q_1(\pi-\chi)-Q_1(\chi) \tag{5}$$

is obtained from the analytic first-order result[1]

$$Q_1(\chi)\equiv\frac{\alpha_S}{\pi}\frac{3-2\zeta}{3[\zeta^9(1-\zeta)]^{1/2}}[3\zeta(2-3\zeta)+2(3-6\zeta+2\zeta^2)\ln(1-\zeta)], \tag{6}$$

where $\zeta\equiv\frac{1}{2}(1-\cos\chi)$. Two computations of the second-order QCD contribution, one numerical[3] and the other based on Monte Carlo parton event generation,[2] agree that $G(\chi)\approx 3$, nearly independent of χ. At the parton level, then, the net effect on the asymmetry from terms of order $\alpha_S{}^2$ is about 10%.

The data will also be compared to predictions of the Lund Monte Carlo[14] (version 5.2) for hadron production in e^+e^- annihilation. This computer program first generates $e^+e^-\to q\bar{q}(g)(g)$ events using the perturbative QCD matrix elements, complete to order $\alpha_S{}^2$ and including virtual corrections.[15] It then simulates the fragmentation of these states into hadrons according to either the Lund model[16] for string fragmentation (STR) or any of a number of incoherent jet (ICJ) models. In the string model the parton system is formally replaced by a relativistic, massless, color-singlet string with diverging end points corresponding to the emerging quark and antiquark; gluons are represented by kinks on the string which carry energy and momentum. The stretching string breaks in a number of places, at each point conserving momentum and producing a quark-antiquark pair at the broken ends. The momentum-carrying string pieces eventually coalesce to form primary hadrons. Conversely, incoherent jet models, based on the work of Field and Feynman[17] and embodied as well in other Monte Carlo programs,[18,19] have the partons fragment independently in the annihilation rest frame; a gluon is treated as a quark-antiquark pair, with its momentum either given entirely to one quark ($g=q$) or shared between both ($g=q\bar{q}$) according to some distribution, e.g., the Altarelli-Parisi function.[20] Momentum conservation needs to be imposed on an ICJ final state in a manifestly *ad hoc* manner; no consensus has emerged as to the most appropriate algorithm to do so. In the "boost" technique,[18] all particles undergo a Lorentz transformation into the zero-momentum frame whereas the "jet" method[19] attempts to equalize the ratios of jet to parent-parton momentum by rescaling the longitudinal components of individual hadron momenta separately within each jet. Different choices for gluon fragmentation and momentum conservation lead to different predictions[21] for $d\Sigma/d\chi$. In particular, to account for a given measured asymmetry, larger values of α_S are required for softer gluon jets ($g=q\bar{q}$ and/or boost) than for harder ones ($g=q$ and/or jet).

In addition to the strong coupling constant α_S, the parton-level event generation requires specification of the infrared cutoff $y_{\min}$. The relative sizes of two-, three-, and four-parton cross sections are defined by the requirement that y, the invariant mass scaled to the center-of-mass energy of any two partons, exceeds $y_{\min}$. The energy-energy correlation asymmetry of the partons generated in this manner approaches the perturbative result of Eq. (4) from above as $y_{\min}\to 0$, but the asymmetry of the final-state hadrons is relatively insensitive[22] to the exact value over the entire χ range for $y_{\min}<0.02$, and for $\chi>40°$ up to $y_{\min}=0.05$ (Ref. 11).

In both STR and ICJ models the momenta of secondary quarks in the jet cascade are generated according to functions with adjustable parameters. The momentum transverse to the initial parton direction forms a Gaussian spectrum of variance $2\sigma_q{}^2$, where previous experiments[23] indicate $\sigma_q\approx 300$ MeV/c. Longitudinal momentum is determined from the fragmentation function[24]

$$f(z)=\frac{1}{z}(1-z)^A e^{-Bm_t{}^2/z}, \tag{7}$$

where z is the fraction of the remaining parton energy plus longitudinal momentum taken by a hadron with transverse mass $m_t\equiv(m^2+p_t{}^2)^{1/2}$. The parameters A and B are constrained to lie on a curve in (A,B) space to maintain the observed multiplicity, a curve that depends on $y_{\min}$, α_S, and σ_q. The energy-energy correlation cross section is very insensitive, however, to the position (A,B) on this curve. Typically the parameter A is fixed at 1.0, and B varied to match the observed charge multiplicity.

Fragmentation alters the asymmetry from the QCD prediction of Eq. (4) in all the models over at least part of the χ range. However, for any one model at fixed $\sqrt{s}$, the asymmetry for $\chi>40°$ has the general shape of Eq. (4), scales nearly linearly with α_S, and has a small sensitivity to variations in other model parameters. Therefore the strong coupling constant can be determined within the context of each model from comparison with the measured asymmetry alone. The predictions for the full correlation differ substantially in shape from model to model, though, opening the possibility that measurement

of $d\Sigma/d\chi$ might distinguish among the fragmentation models.

The implementation of complete second-order QCD in the parton generation of the Lund Monte Carlo (the FKSS[15] scheme with $y_{\min}$ cut) is not unique.[21] Alternatively, the ERT[25] or VGO[26] schemes may be used; these are equivalent[27] to FKSS only when arbitrarily soft gluons are included. In addition, modifications to FKSS have been implemented[12] as the "extended FKSS" scheme. For the soft-gluon cut, Sterman-Weinberg energy-angle (ϵ,Δ) criteria[28] can be used instead of $y_{\min}$ to determine the relative two-, three-, and four-parton cross sections. For nonvanishing infrared cutoffs, required for perturbation theory to be valid, the choice of scheme (ERT, VGO, FKSS, or extended FKSS) and cutoff variable [$y_{\min}$ or (ϵ,Δ)] can affect the postfragmentation cross sections. The extent to which this choice changes $d\Sigma/d\chi$ and $\mathcal{A}(\chi)$ has been only partially investigated, with results shown in Table III and discussed in Sec. V and Ref. 12.

IV. CORRECTIONS AND MEASUREMENT TECHNIQUE

Distortions to the energy-energy correlation cross section arise due to radiation of photons by the initial-state electrons or the final-state partons, detector resolution in angle and energy, and the limited acceptance imposed by solid angle coverage and event selection criteria. Removing these effects facilitates direct comparisons of the data with theoretical predictions and results from other experiments. This unfolding is achieved by multiplying the raw $d\Sigma/d\chi$ by the factor

$$[1+\delta(\chi)](1+\delta_0)\,. \tag{8}$$

The correction $[1+\delta(\chi)]$ is computed as the ratio of a specific hadron-production model's prediction for $d\Sigma/d\chi$ to that obtained from folding the model with a Monte Carlo simulation[9] of initial-state radiation[29] and detector response[30] to hadronic events. The χ-independent shift δ_0 is introduced to preserve the overall normalization of Eq. (2); perfect modeling would have $\delta_0 \equiv 0$. Final-state radiation of photons off quark lines has not been included in the Monte Carlo, but is expected to contribute a negligible amount to the correlation because of the relatively weak electromagnetic couplings.

Because the corrections rely heavily on extremely complex detector modeling that is inevitably imperfect, systematic errors are difficult to estimate *a priori*. Although the MAC detector Monte Carlo yields excellent agreement[9] with the data on many global distributions for hadronic events, such as charge multiplicity, visible energy, and thrust axis direction, subtle inaccuracies known to exist could propagate nontrivial errors into the corrections. In order to probe such subtleties and to establish a reliable estimate of systematic errors, the energy-energy correlation cross section is measured and corrected separately with both the calorimeters and the central drift chamber on the same event sample. For these two independent measurements either the calorimeter hits $\mathbf{E}_i/E_{\rm vis}$ or the charged-particle momenta $\mathbf{p}_i/P_{\rm vis}$ are used as the ϵ_i in the computation of Eq. (1). A typical hadronic event illuminates about 80 channels in the calorimeters, and has about 11 detected charged particles in the drift chamber. For the central shower and central hadron calorimeter, hits without good longitudinal position information from charge division are rejected. For the central drift chamber, only those tracks assigned to the primary vertex and with hits in at least 7 of the 10 layers are accepted (a track with 6 hits is accepted if its momentum exceeds 300 MeV/c). These last requirements ensure that spurious activity and malfunctioning channels in the detector do not affect the measurement.

Figure 1 shows the correction $\delta(\chi)$ for the tracking and calorimetry as well as the resulting fractional corrections $\delta_{\mathcal{A}}(\chi)$ to the raw asymmetry $\mathcal{A}(\chi)$. The differences between the two sets of corrections reflect the many differences in the efficiencies and resolutions (in angle and energy) of the calorimeter and the tracking chamber. All four curves result from smoothing out the fluctuations in the corrections generated from Monte Carlo studies with statistical errors of about 2% in $d\Sigma/d\chi$ and about 15% in $\mathcal{A}(\chi)$. The errors remaining in the curves of Fig. 1 due to this smoothing procedure are estimated to be approximately $\pm 1.5\%$ in $\delta(\chi)$ and $\pm 10\%$ in $\delta_{\mathcal{A}}(\chi)$. Within the range $30^\circ < \chi < 150^\circ$ all four curves in Fig. 1 are slowly varying and of moderate magnitude, in sharp contrast to the rapidly changing behavior outside this region. Hence imperfect modeling leads to differences between the two measurement techniques, as well as systematic errors, that can be expected to be greater for very large or very small

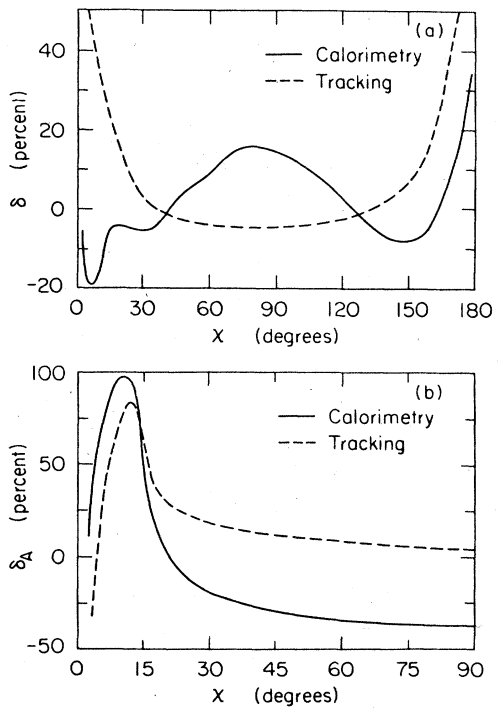

FIG. 1. (a) The fractional corrections $\delta(\chi)$ applied to the raw energy-energy correlation. (b) The fractional corrections $\delta_{\mathcal{A}}(\chi)$ applied to the raw asymmetry. In both figures the solid (dashed) curves apply to the measurement using the calorimeters (central drift chamber).

correlation angles than for intermediate values. The values of the constant normalization shifts δ_0 for the calorimetry and tracking are 0.8% and 1.9%, respectively, indicating that the hadronic event modeling reproduces the general χ variation of the data very well.

In principle the corrections can depend on the model used to generate the hadronic events. The corrections for both measurement techniques shown in Fig. 1 are identical for events generated with string fragmentation and with incoherent jet formation, within the smoothing errors quoted above.

V. RESULTS AND CONCLUSIONS

Figure 2 shows the corrected distributions for the two measurements. The discrepancy between them grows from $\sim 3\%$ for $\chi \approx 90°$ to a maximum of $\sim 7\%$ for larger or smaller χ values, the trend anticipated from the shapes of the corrections. Interpreting the discrepancies between the two sets of data as a gauge of the systematic errors, attributable to inaccuracies in detector modeling, the best measure of the energy-energy correlation cross section and its asymmetry is taken as the arithmetic mean of the calorimetry and tracking results. The total error in each χ bin is computed by summing in quadrature the larger of the two statistical errors and a systematic uncertainty; the latter consists of a Monte Carlo correction error [1.5% for $d\Sigma/d\chi$ and 10% for $\mathcal{A}(\chi)$] added in quadrature with half the difference between the calorimetry and tracking values. The errors for the asymmetry $\mathcal{A}(\chi)$ are calculated separately to avoid the systematic errors in $d\Sigma/d\chi$ that are symmetric about $\chi = 90°$. The numerical values are given in Table I and are plotted in Fig. 3. The statistical errors in $d\Sigma/d\chi$ are smaller than the systematic contributions and the total error is 3–4 % over most of the χ range. The total error in the asymmetry for $\chi > 40°$ contributes only 5% to the determination of α_S within any model.

An attempt has been made to vary the parameters in the Monte Carlo models discussed above to obtain agreement with the data. The procedure to do so is iterative and consists of adjusting (i) α_S, in steps of 0.005, to match the measured $\mathcal{A}(\chi)$ for $\chi > 40°$, with fixed $y_{\min} = 0.015$; (ii) the fragmentation-function parameter B, in steps of

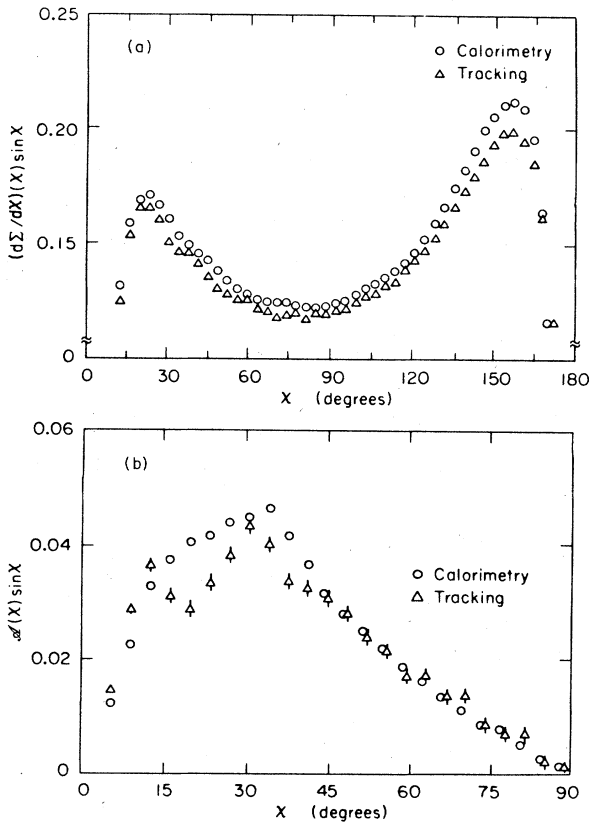

FIG. 2. (a) The corrected energy-energy correlation $d\Sigma/d\chi$. (b) The corrected asymmetry $\mathcal{A}(\chi)$. In both figures the open circles (triangles) represent the measurement of the calorimeters (central drift chamber). The data are scaled by $\sin\chi$ to facilitate presentation on a linear scale. Only the statistical errors of the data are shown.

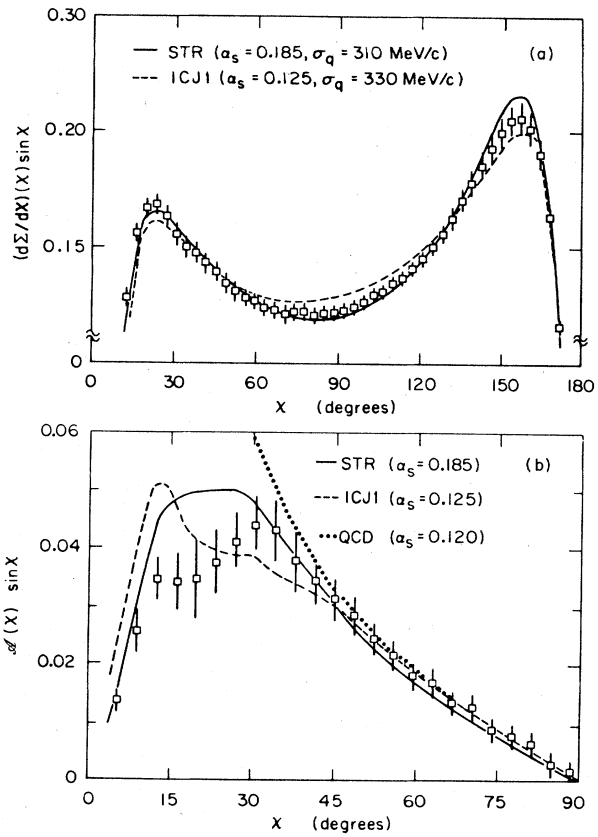

FIG. 3. (a) The corrected energy-energy correlation $d\Sigma/d\chi$ and (b) the corrected asymmetry $\mathcal{A}(\chi)$, both multiplied by $\sin\chi$, as determined from the average of the results from the calorimetry and tracking shown in Fig. 2. The error bars include the statistical error of the data, a contribution from the corrections, and a systematic error estimated from the differences between the two measurements as described in the text. The curves show the predictions of the best-fit string (STR) and incoherent jet (ICJ1) fragmentation models, using the Lund Monte Carlo and FKSS scheme, with the parameters shown in Table II. The dotted curve in (b) shows the result from fitting the asymmetry to second-order perturbative QCD according to Eq. (4).

TABLE I. The numerical values of the corrected energy-energy correlation $d\Sigma/d\chi$ and asymmetry $\mathscr{A}(\chi)$ with combined statistical and systematic errors.

χ (deg)	$\frac{d\Sigma}{d\chi}(\chi)$ (mrad^{-1})	$\frac{d\Sigma}{d\chi}(\pi-\chi)$ (mrad^{-1})	$\mathscr{A}(\chi)$ (mrad^{-1})
1.8	1624±305	241±16	−1383±321
5.4	430±21	575±13	145±20
9.0	580±25	743±13	164±26
12.6	589±19	747±15	158±19
16.2	560±13	682±24	122±17
19.8	493±10	595±25	102±21
23.4	424±10	518±19	94±15
27.0	360±10	451±16	90±12
30.6	306±12	392±14	86±10
34.2	267±8	343±13	77±10
37.8	241±5	302±11	61±9
41.4	217±5	269±8	52±7
45.0	197±6	241±7	44±5
48.6	180±6	217±6	37±4
52.2	167±5	197±5	31±4
55.8	155±4	182±4	26±3
59.4	148±3	169±4	21±3
63.0	139±4	158±3	19±3
66.6	134±3	149±4	15±2
70.2	129±4	143±3	13±3
73.8	127±4	136±4	9±2
77.4	125±3	133±3	8±2
81.0	122±4	128±3	6±2
84.6	122±3	125±3	2±2
88.2	122±3	123±3	1±2

0.01, to yield the correct mean charge multiplicity, with fixed $A=1.0$; and (iii) σ_q, in steps of 10 MeV/c, to minimize the χ^2 for the fit of the model's $d\Sigma/d\chi$ to the data. Depending on the initial values used, a few iterations over these procedures are required to obtain consistency, because the asymmetry depends weakly on σ_q and the charge multiplicity depends weakly on both α_S and σ_q. The relative χ^2 values obtained with different models are more significant than absolute values because the bin-to-bin correlations of the systematic errors have not been included. The best-fit parameters for five models are shown in Table II and two of the cross sections (STR and ICJ1) are plotted in Fig. 3. The row and curve labeled QCD is obtained from fitting the measured $\mathscr{A}(\chi)$ to Eq. (4), yielding[31] α_S (QCD)=0.120±0.006. The errors assigned to α_S for the five models include the measurement error of 5% added in quadrature with a 5% Monte Carlo contribution. The latter accounts for the finite step size and slightly different values of α_S that would result with other compatible choices of the parameters [e.g., other $y_{\min}$, σ_q, or (A,B) values].

The string model reproduces the measured $d\Sigma/d\chi$ with considerably smaller χ^2 than incoherent jet fragmentation (each ICJ model has a χ^2 more than 2.8 times larger). All four ICJ models predict higher values near $\chi=90°$ than the data and lower near $\chi=30°$ or 150°. Any ICJ prediction for $d\Sigma/d\chi$ can be shifted slightly up or down (nearly uniformly over the range $20°<\chi<160°$) by varying $y_{\min}$ and/or σ_q without significantly improving the fit to the data. The data are systematically shifted away from the

TABLE II. The parameters resulting from fitting the data to five Monte Carlo models of QCD and fragmentation and to perturbative QCD (row 1). For all cases except QCD in row 1, which uses the analytic formula of Eq. (4), the FKSS scheme in the Lund Monte Carlo was used, with $y_{\min}=0.015$ and the fragmentation parameter A fixed at 1.0. For the $g=q\bar{q}$ cases, the quark and antiquark share the gluon momentum according to the Altarelli-Parisi function.

Label	Gluon fragmentation	p conservation	B (GeV^{-2})	σ_q (MeV/c)	α_S from $\mathscr{A}(\chi)$	χ^2 for $d\Sigma/d\chi$
QCD	None				0.120±0.006	
STR	String		0.67	310	0.185±0.013	35
ICJ1	$g=q$	Boost	0.47	330	0.125±0.009	136
ICJ2	$g=q\bar{q}$	Boost	0.60	320	0.140±0.010	201
ICJ3	$g=q$	Jet	0.43	360	0.105±0.007	98
ICJ4	$g=q\bar{q}$	Jet	0.50	350	0.110±0.008	142

string model prediction by small amounts near $\chi = 30°$ and 150°, a feature reflected more strongly in the asymmetry, but it is unclear whether this represents an inadequacy in the corrections or a deficiency in the model. Indeed, for small angles in the asymmetry, the corrections are large and changing rapidly, and the model displays considerable sensitivity to $y_{\min}$ (Ref. 11).

All the models represent the measured asymmetry well for $\chi > 30°$; the value of α_S for the string model is 0.185 ± 0.013, and for ICJ models varies from 0.105 to 0.140 (± 0.01), depending on the choice of gluon fragmentation and momentum conservation scheme. If only first-order perturbative QCD were used in the Monte Carlo calculations, the values of α_S would be larger by about 10% for incoherent jet models and by about 30% for the string model. This suggests that nontrivial corrections are likely to occur at higher orders than $\alpha_S{}^2$, especially for string fragmentation. All the models predict a higher asymmetry for $\chi < 30°$ than observed. This is the region where the corrections are large and changing rapidly, an effect that is perhaps not properly included in the errors assigned to the asymmetry.

The above conclusions are unchanged when the tracking and calorimetry data are analyzed separately. The two sets of independently measured points shown in Fig. 2 are identical, within errors, for the asymmetry $\mathscr{A}(\chi)$ for $\chi > 40°$, so that the best-fit value for α_S in any model is virtually the same as shown in Table II; furthermore, they are similar in the shape of $d\Sigma/d\chi$ for $20° < \chi < 160°$, thus leading to the same conclusion regarding the preference of the overall fit for string fragmentation over ICJ models. The different absolute levels of $d\Sigma/d\chi$ in the two data sets do result in different values of σ_q and B. In each fragmentation model, the calorimetry (tracking) data yield best-fit values for σ_q about 25 MeV/c larger (smaller) and for B about 0.04 GeV^{-2} smaller (larger) than the combined-data fits of Table II.

Table III briefly summarizes experimental results on energy-energy correlations in high-energy e^+e^- annihilation into hadrons. The preference for the string model seen in this experiment was also observed in the JADE[11] analysis, but Mark J[7] obtained equally good fits with the string model and an incoherent jet model ($g = q\bar{q}$ and boost, corresponding to ICJ2 in Tables II and III). The other experiments did not present data for $d\Sigma/d\chi$. The α_S values of this experiment obtained from the asymmetry at large correlation angles are consistent with those found by JADE,[11] CELLO,[10] and TASSO,[12] but are about 20% larger than those determined by Mark J.[7] At least part of this difference can be attributed to different treatments of second-order QCD at the parton generation level in the Monte Carlos. This effect is most apparent in the last column of Table III where the direct comparison of extended FKSS with ERT from Ref. 12 is given, which shows that when (ϵ, Δ) cuts are used, systematically lower values of α_S are obtained with ERT than with extended FKSS.

In conclusion, the energy-energy correlation cross section has been measured with high statistics and compared with models of second-order QCD and fragmentation. Two analyses of the data use independent measuring devices, the drift chamber and the calorimeters, and give similar results when separately corrected for detector bias and initial-state radiation. Differences between the two results are used to estimate systematic errors in the measurements and corrections. Values of the strong coupling constant as a parameter in Monte Carlo models are determined from the asymmetry in the correlation. A much better description of the data is obtained with the string fragmentation scheme than with incoherent jet models.

TABLE III. A brief summary of results on energy-energy correlations from five experiments is shown. The symbol "· · ·" signifies that an appropriate result was not available for that table entry. Other symbols and abbreviations are explained in the text or Table II. Errors for the α_S values quoted have been omitted, but are all in the range of $\pm(5-15)\%$.

Experiment	MAC	JADE	Mark J	CELLO	TASSO
Reference	This article	11	7	10	12
$\sqrt{s}$ (GeV)	29	34	34	34	34
Measured $d\Sigma/d\chi$?	Yes	Yes	Yes	No	No
$d\Sigma/d\chi$ best-fit model	STR	STR	STR&ICJ2	· · ·	· · ·
Second-order QCD	FKSS $y_{\min}=0.015$	FKSS $y_{\min}=0.0125$	ERT $\epsilon=0.1$, $\Delta=13°$	FKSS $y_{\min}=0.03$	Extended FKSS/ERT $\epsilon=0.2$, $\Delta=40°$
α_S from $\mathscr{A}(\chi)$ in STR	0.185	0.165	0.14	0.19	0.190/0.159
α_S from $\mathscr{A}(\chi)$ in ICJ1	0.125	0.123	· · ·	0.15	0.139/0.117
α_S from $\mathscr{A}(\chi)$ in ICJ2	0.140	0.140	0.12	· · ·	0.157/0.127
α_S from $\mathscr{A}(\chi)$ in ICJ3	0.105	0.112	· · ·	0.12	· · ·
α_S from $\mathscr{A}(\chi)$ in ICJ4	0.110	0.115	· · ·	· · ·	· · ·

ACKNOWLEDGMENTS

The authors gratefully acknowledge the continuing efforts of the PEP Division in operating the machine efficiently. We also thank S. D. Ellis for many illuminating conversations and constant encouragement, and A. Petersen for several useful discussions concerning the Lund Monte Carlo and the JADE results. We are also grateful for the efforts of the engineers, technicians, and staff of the collaborating institutions in the construction and operation of the experiment. This work was supported in part by the Department of Energy, under Contract numbers DE-AC02-81ER40025 (CU), DE-AC03-76SF00515 (SLAC), and DE-AC02-76ER00881 (UW), and by the National Science Foundation under Contract numbers NSF-PHY82-15133 (UH), NSF-PHY82-15413, and NSF-PHY82-15414 (NU), NSF-PHY80-06504 (UU), and by INFN.

---

*Present address: CERN, CH-1211, Geneva 23, Switzerland.

†Present address: Los Alamos National Laboratory, Los Alamos, New Mexico 87545.

‡Present address: Lawrence Berkeley Laboratory, Berkeley, Calfornia 94720.

§Permanent address: CERN, CH-1211, Geneva 23, Switzerland.

**Present address: Department of Physics, Chungnam National University, Daejeon, Korea.

††Present address: Laboratory of Nuclear Studies, Cornell University, Ithaca, New York 14853.

[1]C. L. Basham, L. S. Brown, S. D. Ellis, and S. T. Love, Phys. Rev. D **17**, 2298 (1978); Phys. Rev. Lett. **41**, 1585 (1978); Phys. Rev. D **19**, 2018 (1979).

[2]A. Ali and F. Barreiro, Nucl. Phys. **B236**, 269 (1984).

[3]D. G. Richards, W. J. Stirling, and S. D. Ellis, Phys. Lett. **119B**, 193 (1982).

[4]Ch. Berger *et al.*, Phys. Lett. **99B**, 292 (1981).

[5]H.-J. Behrend *et al.*, Z. Phys. C **14**, 95 (1982).

[6]D. Schlatter *et al.*, Phys. Rev. Lett. **49**, 521 (1982).

[7]B. Adeva *et al.*, Phys. Rev. Lett. **50**, 2051 (1983).

[8]R.-Y. Zhu, MIT-LNS Report No. RX-1033, 1983, Ph.D. thesis.

[9]B. K. Heltsley, University of Wisconsin—Madison Report WISC-EX-83/233, 1983, Ph.D. thesis.

[10]H.-J. Behrend *et al.*, Phys. Lett. **138B**, 311 (1984).

[11]W. Bartel *et al.*, Z. Phys. C **25**, 231 (1984).

[12]M. Althoff *et al.*, Report No. DESY 84-057, 1984 (unpublished).

[13]MAC Collaboration, in *Proceedings of the International Conference on Instrumentation for Colliding Beams,* edited by W. Ash (SLAC Report No. 250, 1982), p. 174; G. Gidal, B. Armstrong, and A. Rittenberg, LBL Report No. LBL-91, 1983 (unpublished).

[14]T. Sjöstrand, Comp. Phys. Commun. **27**, 243 (1982); **28**, 229 (1983).

[15]K. Fabricius, G. Kramer, G. Schierholz, and I. Schmitt, Z. Phys. C **11**, 315 (1982).

[16]B. Andersson, G. Gustafson, G. Ingleman, and T. Sjöstrand, Phys. Rep. **97**, 33 (1983).

[17]R. D. Field and R. P. Feynman, Phys. Rev. D **15**, 2590 (1977); Nucl. Phys. **B136**, 1 (1978).

[18]A. Ali, E. Pietarinen, and J. Willrodt, Report No. DESY T-80/01, 1980 (unpublished); A. Ali, E. Pietarinen, G. Kramer, and J. Willrodt, Phys. Lett. **93B**, 155 (1980).

[19]P. Hoyer, P. Osland, H. G. Sander, T. F. Walsh, and P. M. Zerwas, Nucl. Phys. **B161**, 349 (1979).

[20]G. Altarelli and G. Parisi, Nucl. Phys. **B126**, 298 (1977).

[21]T. Sjöstrand, Report No. DESY 84-023 (unpublished).

[22]T. Sjöstrand, Report No. DESY 84-019 (unpublished).

[23]G. Wolf, Report No. DESY 83-096 (unpublished).

[24]B. Andersson, G. Gustafson, and B. Söderberg, Z. Phys. C **20**, 317 (1983).

[25]R. K. Ellis, D. A. Ross, and A. E. Terrano, Nucl. Phys. **B178**, 421 (1981).

[26]J. A. M. Vermaseren, K. J. F. Gaemers, and S. J. Oldham, Nucl. Phys. **B187**, 301 (1981).

[27]T. Gottschalk, Phys. Lett. **109B**, 331 (1982); F. Gutbrod, G. Kramer, and G. Schierholz, Z. Phys. C **21**, 235 (1984).

[28]G. Sterman and S. Weinberg, Phys. Rev. Lett. **39**, 1436 (1977).

[29]F. A. Berends, R. Kleiss, and S. Jadach, Nucl. Phys. **B202**, 63 (1982).

[30]Electromagnetic showers were simulated by the EGS code, described in R. L. Ford and W. R. Nelson, Stanford Linear Accelerator Center Report No. SLAC-0210, 1978 (unpublished); and hadron cascades by HETC, described in the report of T. W. Armstrong, in *Computer Techniques in Radiation Transport and Dosimetry,* edited by W. R. Nelson and T. M. Jenkins (Plenum, New York, 1980).

[31]In order to fit the measured $d\Sigma/d\chi$ using the analytic QCD prediction, terms accounting for fragmentation must be also included. Such analytic approaches are discussed in Refs. 5, 6, and 9.